

Properties of Light Flavour Baryons in Hypercentral quark model

Kaushal Thakkar*, Bhavin Patel†, Ajay Majethiya‡ and P.C.Vinodkumar*

*Department of Physics, Sardar Patel University, Vallabh Vidyanagar- 388 120,

† LDRP, Gandhinagar, Gujarat, ‡ KITRC, Kalol, Gujarat, INDIA.

E-mail: kaushal21185@yahoo.co.in

Abstract.

The light flavour baryons are studied within the quark model using the hypercentral description of the three-body system. The confinement potential is assumed as hypercentral coulomb plus power potential ($hCPP_\nu$) with power index ν . The masses and magnetic moments of light flavour baryons are computed for different power index, ν starting from 0.5 to 1.5. The predicted masses and magnetic moments are found to attain a saturated value with respect to variation in ν beyond the power index $\nu > 1.0$. Further we computed transition magnetic moments and radiative decay width of light flavour baryons. The results are in good agreement with known experimental as well as other theoretical models.

PACS numbers: 12.39.Jh, 12.39.Pn, 13.40.Em, 13.40.Hq

1. Introduction

Baryons are not only the interesting systems to study the quark dynamics and their properties but are also interesting from the point of view of simple systems to study three body interactions. In the last two decades, there has been great advancement in the study of baryon properties. The ground state masses and magnetic moments of many low lying baryons have been measured experimentally. The magnetic moments of all octet baryons ($J^P = \frac{1}{2}^+$) are known accurately except for Σ^0 which has a life time too short. For the decuplet baryons ($J^P = \frac{3}{2}^+$), the experimental measurements are poor as they have very short life times due to available strong interaction decay channels. The Ω^- is an exception as it is composed of three s quarks which decays via weak interaction causing longer life time for it [1]. The Δ particles are produced in scattering the pion, photon, or electron beams off a nucleon target. High precision measurements of the $N \rightarrow \Delta$ transition by means of electromagnetic probes became possible with the advent of the new generation of electron beam facilities such as LEGS, BATES, ELSA, MAMI, and those at the Jefferson Lab. Many such experimental programs devoted to the study of electromagnetic properties of the Δ have been reported in the past few years [2, 3, 4]. The electromagnetic transition of $\Delta \rightarrow N\gamma$ have been the subject of intense study [5, 6, 7, 8, 9, 10]. The experimental information provides new incentives for theoretical study of these observables.

Theoretically, there exist serious discrepancies between the quark model and experimental results particularly in the predictions of their magnetic moments [11, 12, 13]. Prediction of transition magnetic moments between the decuplet to octet ($\frac{3}{2}^+ \rightarrow \frac{1}{2}^+$) is as important as the prediction of the masses and magnetic moments of the baryons (octet and decuplet) for testing of any model hypothesis and understanding the dynamics of quarks and meaning of the constituent mass of the quarks in the hadronic scale. Various attempts including lattice QCD (Latt) [14, 15, 16], chiral perturbation theory (χ PT) [17, 18, 19, 20, 21], relativistic quark model (RQM) [22, 23], non relativistic quark model (NRQM) [24], QCD sum rules (QCDSR) [12, 13, 25, 26], chiral quark soliton model (χ QSM) [27, 28], chiral constituent quark model (χ CQM) [29], chiral bag model (χ B) [30], cloudy bag model [31], quenched lattice gauge theory [32] etc., have been tried, but with partial success.

The importance of three body interaction in the description of baryon was felt in many cases. In this context it is found that the six dimensional hyper central model with coulomb plus power potential ($hCPP_\nu$) is successful in predicting the masses and magnetic moments of heavy flavour baryons (baryon containing charm or beauty quarks) [33, 34]. Unlike in the case of many other potential models, in the $hCPP_\nu$ model, the confinement potential expressed in terms of the three body hyper spherical co-ordinate is able to account for the three body effects.

Accordingly, in this paper we extend the $hCPP_\nu$ model in the light flavour baryonic sector to compute the masses, magnetic moments of octet and decuplet baryons. We also study the electromagnetic transition and radiative decay width of those baryons. In section 2 the hypercentral scheme and a brief introduction of $hCPP_\nu$ potential employed for the present study are described. Section 3 describes the computational details of the magnetic moments of octet and decuplet baryons and the $\frac{3}{2}^+ \rightarrow \frac{1}{2}^+$ transition magnetic moments. Section 4 describes the radiative decay widths for those transition. In section 5, we discuss our results while comparing with other theoretical predictions and experimental results and draw important conclusions.

2. Hyper Central Scheme for Baryons

Quark model description of baryons is a simple three body system of interest. Generally the phenomenological interactions among the three quarks are studied using the two-body quark potentials such as the Isgur Karl Model [35], the Capstick and Isgur relativistic model [36, 37], the Chiral quark model [38], the Harmonic Oscillator model [39, 40] etc. The three-body effects are incorporated in such models through two-body and three-body spin-orbit terms [33, 41]. The Jacobi Co-ordinates to describe baryon as a bound state of three different constituent quarks is given by [42]

$$\vec{\rho} = \frac{1}{\sqrt{2}}(\vec{r}_1 - \vec{r}_2) ; \vec{\lambda} = \frac{(m_1\vec{r}_1 + m_2\vec{r}_2 - (m_1 + m_2)\vec{r}_3)}{\sqrt{m_1^2 + m_2^2 + (m_1 + m_2)^2}} \quad (1)$$

Such that

$$m_\rho = \frac{2 m_1 m_2}{m_1 + m_2} ; m_\lambda = \frac{2 m_3 (m_1^2 + m_2^2 + m_1 m_2)}{(m_1 + m_2)(m_1 + m_2 + m_3)} \quad (2)$$

Here m_1 , m_2 and m_3 are the constituent quark mass parameters.

In the hypercentral model, we introduce the hyper spherical coordinates which are given by the angles

$$\Omega_\rho = (\theta_\rho, \phi_\rho) ; \Omega_\lambda = (\theta_\lambda, \phi_\lambda) \quad (3)$$

together with the hyper radius, x and hyper angle ξ respectively as,

$$x = \sqrt{\rho^2 + \lambda^2} ; \xi = \arctan\left(\frac{\rho}{\lambda}\right) \quad (4)$$

The model Hamiltonian for baryons can now be expressed as

$$H = \frac{P_\rho^2}{2 m_\rho} + \frac{P_\lambda^2}{2 m_\lambda} + \frac{P_R^2}{2 M} + V(\rho, \lambda) = \frac{P_x^2}{2 m} + V(x) \quad (5)$$

Here the potential $V(x)$ is not purely a two body interaction but it contains three-body effects also. The three body effects are desirable in the study of hadrons since the non-abelian nature of QCD leads to gluon-gluon couplings which produce three-body forces

[43]. Using hyperspherical coordinates, the kinetic energy operator $\frac{P_x^2}{2m}$ of the three-body system can be written as

$$\frac{P_x^2}{2m} = \frac{-1}{2m} \left(\frac{\partial^2}{\partial x^2} + \frac{5}{x} \frac{\partial}{\partial x} - \frac{L^2(\Omega_\rho, \Omega_\lambda, \xi)}{x^2} \right) \quad (6)$$

Where $L^2(\Omega_\rho, \Omega_\lambda, \xi)$ is the quadratic Casimir operator of the six dimensional rotational group $O(6)$ and its eigen functions are the hyperspherical harmonics, $Y_{[\gamma]l_\rho l_\lambda}(\Omega_\rho, \Omega_\lambda, \xi)$ satisfying the eigenvalue relation

$$L^2 Y_{[\gamma]l_\rho l_\lambda}(\Omega_\rho, \Omega_\lambda, \xi) = \gamma(\gamma + 4) Y_{[\gamma]l_\rho l_\lambda}(\Omega_\rho, \Omega_\lambda, \xi) \quad (7)$$

Here γ is the grand angular quantum number and it is given by $\gamma = 2\nu + l_\rho + l_\lambda$, and $\nu = 0, 1, \dots$ and l_ρ and l_λ being the angular momenta associated with the ρ and λ variables.

If the interaction potential is hyper spherical such that the potential depends only on the hyper radius x , then the hyper radial schrodinger equation corresponds to the hamiltonian given by Eqn.(5) can be written as

$$\left[\frac{d^2}{dx^2} + \frac{5}{x} \frac{d}{dx} - \frac{\gamma(\gamma + 4)}{x^2} \right] \phi_\gamma(x) = -2m[E - V(x)] \phi_\gamma(x) \quad (8)$$

where γ is the grand angular quantum number.

For the present study we consider the hyper central potential $V(x)$ as the hyper coulomb plus power (hCPP ν) form given by [33, 34, 44]

$$V(x) = -\frac{\tau}{x} + \beta x^\nu + \kappa + V_{spin} \quad (9)$$

In the above equation the spin independent terms correspond to confinement potential in the hyperspherical co-ordinates. The form of the potential though hyper central, belong to a generality of potentials of the form $-Ar^\alpha + kr^\epsilon + V_0$ where A, k, α and ϵ are non negative constants where as V_0 can have either sign. There are many attempts with different choices of α and ϵ to study the hadron properties [45]. For example, Cornell potential has $\alpha = \epsilon = 1$, Lichtenberg potential has $\alpha = \epsilon = 0.75$. Song-Lin potential has $\alpha = \epsilon = 0.5$ and the Logarithmic potential of Quigg and Rosner corresponds to $\alpha = 0$, $\epsilon \rightarrow 0$ [45]. Martin potential corresponds to $\alpha=0$, $\epsilon = 0.1$ [45] while Grant, Rosner and Rynes potential corresponds to $\alpha = 0.045$, $\epsilon = 0$; Heikkilä, Törnquist and Ono potential corresponds to $\alpha = 1$, $\epsilon = 2/3$ [46]. Potentials in the region $0 \leq \alpha \leq 1.2$, $0 \leq \epsilon \leq 1.1$ of $\alpha - \epsilon$ values are also been explored [47]. So it is important to study the behavior of different potential scheme with different choices of α and ϵ to know the dependence of their parameters to the hadron properties. The spin independent part of potential defined by Eqn.(9) corresponds to $\alpha = 1$ and $\epsilon = \nu$. Here τ of the hyper-coulomb, β of the confining term and κ are the model parameters. The parameter τ is related to the strong running coupling constant α_s as [33, 34]

$$\tau = \frac{2}{3} b \alpha_s \quad (10)$$

where b is the model parameter, $\frac{2}{3}$ is the color factor for the baryon. The potential parameters treated here are similar to the one employed for the study of heavy flavour baryons [33, 34]. The strong running coupling constant is computed using the relation

$$\alpha_s = \frac{\alpha_s(\mu_0)}{1 + \frac{33-2n_f}{12\pi}\alpha_s(\mu_0)\ln(\frac{\mu}{\mu_0})} \quad (11)$$

where $\alpha_s(\mu_0 = 1\text{GeV}) \approx 0.6$ is considered in the present study. The spin dependent part of the three body interaction potential of Eqn.(9) is taken as [33, 41]

$$V_{spin}(x) = -\frac{1}{4}\alpha_s \frac{e^{-\frac{x}{x_0}}}{xx_0^2} \sum_{i<j} \frac{\vec{\sigma}_i \cdot \vec{\sigma}_j}{6m_i m_j} \vec{\lambda}_i \cdot \vec{\lambda}_j \quad (12)$$

where, x_0 is the hyperfine parameter of the model.

The six dimensional radial Schrodinger equation described by Eqn.(8) has been solved in the variational scheme with the hyper coulomb trial radial wave function given by [43]

$$\psi_{\omega\gamma} = \left[\frac{(\omega - \gamma)!(2g)^6}{(2\omega + 5)(\omega + \gamma + 4)!} \right]^{\frac{1}{2}} (2gx)^\gamma e^{-gx} L_{\omega-\gamma}^{2\gamma+4}(2gx) \quad (13)$$

The wave function parameter g and hence the energy eigen value are obtained by applying virial theorem for a chosen potential index ν .

The baryon masses are determined by the sum of the model quark masses plus kinetic energy, potential energy and the spin hyperfine interaction as

$$M_B = \sum_i m_i + \langle H \rangle \quad (14)$$

For the present calculations, we have employed the same mass parameters of the light flavour quarks ($m_u = 338$ MeV, $m_d = 350$ MeV, $m_s = 500$ MeV) as used in [33]. We fix other parameters (b of Eqn.(10) and x_0 of Eqn.(12)) of the model for each choice of ν using the experimental center of weight (spin-average) mass and hyper fine splitting of the octet decuplet baryons. The procedure is repeated for different choices of ν and the computed masses of octet and decuplet baryons are listed in Table 1 and Table 2 respectively.

3. Magnetic moments of light baryons

Now the magnetic moment of the baryons are computed in terms of its quarks spin-flavour wave function of the constituent quarks as

$$\mu_B = \sum_i \langle \phi_{sf} | \mu_i \vec{\sigma}_i | \phi_{sf} \rangle \quad (15)$$

where

$$\mu_i = \frac{e_i}{2m_i} \quad (16)$$

Here e_i and σ_i represents the charge and the spin of the quark constituting the baryonic state and $|\phi_{sf}\rangle$ represents the spin-flavour wave function of the respective baryonic state as listed in [48]. Here, m_i the mass of the i^{th} quark in the three body baryon is taken as an effective mass of the constituting quarks as their motions are governed by the three body force described through the $hCPP_\nu$ potential appeared in the hamiltonian 5. Accordingly, within the baryon the mass of the quarks may get modified due to its binding interactions with other two quarks. We account for this bound state effect by replacing the mass parameter m_i of Eqn.(16) by defining an effective mass to the bound quarks, m_i^{eff} as given by [33, 34, 44]

$$m_i^{eff} = m_i \left(1 + \frac{\langle H \rangle}{\sum_i m_i} \right) \quad (17)$$

such that $M_B = \sum_{i=1}^3 m_i^{eff}$. The computations are repeated for the different choices of the flavour combinations of qqq (q = u, d, s). The computed magnetic moments of the octet and decuplet baryons are listed in Table 3 and 4 respectively.

4. Radiative Decay Width

The radiative decays of baryons provide much better understanding of the underlying structure of baryons and the dependence on the constituent quark mass. Though the non-relativistic model of Isgur and Karl successfully predicted the electromagnetic properties of the low lying octet baryons but it fails to provide a good description of the radiative decay of the decuplet baryons [35, 50]. Thus, the successful prediction of the electromagnetic properties of octet baryons as well as the decuplet baryons become detrimental for all the phenomenological models. The radiative decay width of the baryons can be computed using the relation given by [44]

$$\Gamma_R = \frac{q^3}{4\pi} \frac{2}{2J+1} \frac{e^2}{m_p^2} |\mu_{\frac{3}{2}^+ \rightarrow \frac{1}{2}^+}|^2 \quad (18)$$

where m_p is the proton mass, $\mu_{\frac{3}{2}^+ \rightarrow \frac{1}{2}^+}$ is the radiative transition magnetic moments, q is the photon energy and is given by $M_{\frac{3}{2}^+} - M_{\frac{1}{2}^+}$.

The transition magnetic moments for $\frac{3}{2}^+ \rightarrow \frac{1}{2}^+$ are computed as

$$\mu_{\frac{3}{2}^+ \rightarrow \frac{1}{2}^+} = \sum_i \langle \phi_{sf}^{\frac{3}{2}^+} | \mu_i \vec{\sigma}_i | \phi_{sf}^{\frac{1}{2}^+} \rangle \quad (19)$$

$|\phi_{sf}^{\frac{3}{2}^+}\rangle$ represent the spin flavour wave function of the quark composition for the respective decuplet baryons while $|\phi_{sf}^{\frac{1}{2}^+}\rangle$ represent the spin flavour wave function of the quark composition for the octet baryons. The value of μ_i is given by Eqn.(16) and the m_i^{eff}

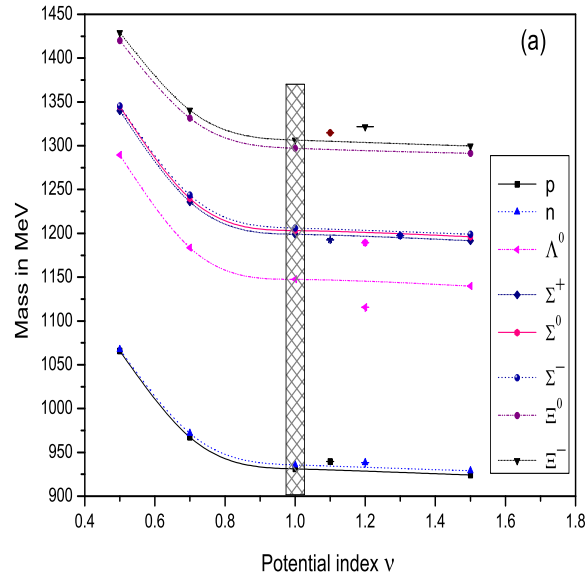


Figure 1. Variation of octet baryon masses with respect to potential index ν . Experimental masses are shown with error bar. The shaded region show minimum root mean square deviation with experimental results.

for the transition is calculated using geometric mean of effective quark masses of decuplet and octet baryons as given by [49]

$$m_i^{eff} = \sqrt{m_{i(\frac{3}{2}^+)}^{eff} m_{i(\frac{1}{2}^+)}^{eff}} \quad (20)$$

The calculated transition magnetic moments are listed in Table 5

We also calculate the branching ratio $\frac{\Gamma_R}{\Gamma(Baryon)}$ using the experimental total decay width $\Gamma(Baryon)$ of the respective decuplet baryons. The computed values of radiative decay width and the branching ratio for different choices of the potential power indices are listed in Table 6.

5. Results and Discussion

The masses of octet and decuplet baryons in the hypercentral coulomb plus power potential ($hCPP_\nu$) model with the different choices of potential index ν have been studied. Fig.(1) and Fig.(2) show the behaviour of the predicted masses of the octet and decuplet baryons with the potential index ν in the range, $0.5 \leq \nu \leq 1.5$. The trend lines here show saturation of the masses beyond $\nu \geq 1.0$. The shaded regions in Fig.(1) and in Fig.(2) show the neighbourhood region of ν at which the predicted masses are having minimum root mean square deviation with the experimental masses.

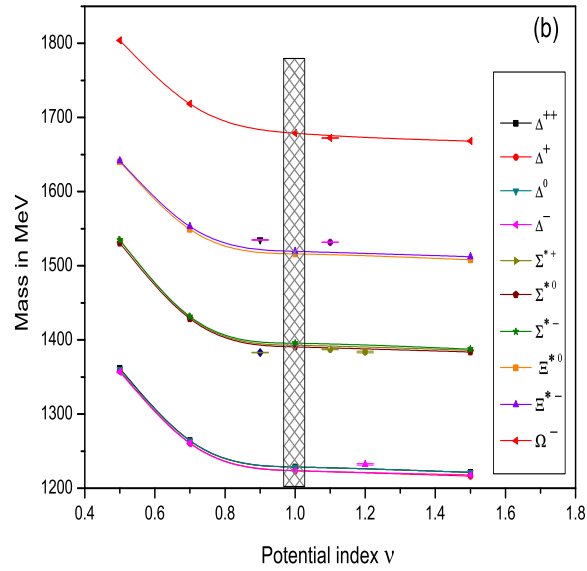


Figure 2. Variation of decuplet baryon masses with respect to potential index ν . Experimental masses are shown with error bar. The shaded region show minimum root mean square deviation with experimental results.

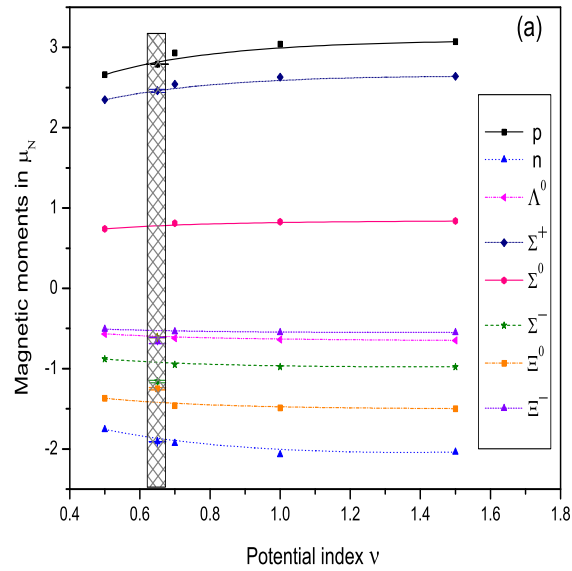


Figure 3. Behaviour of the magnetic moments of octet baryons with respect to potential index ν . The known experimental values are shown with error bar. The shaded region show minimum root mean square deviation with experimental results.

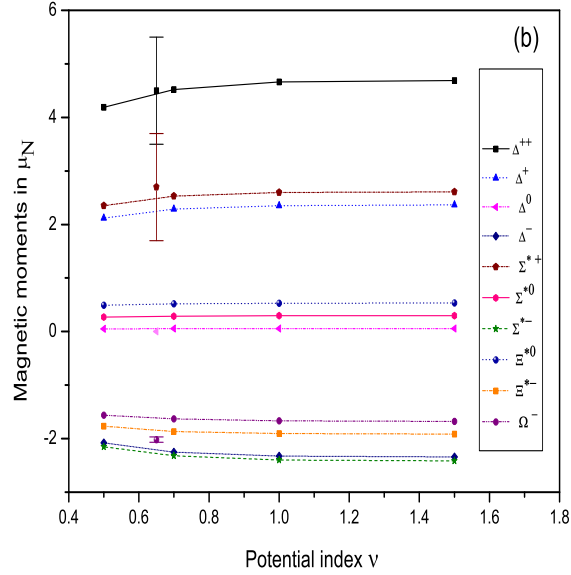


Figure 4. Behaviour of the magnetic moments of decuplet baryons with respect to potential index ν . The known experimental values are shown with error bar.

Table 1. Masses of octet baryons ($J^P = \frac{1}{2}^+$)

hCPP $_{\nu}$	Model	Baryon	Octet Mass(MeV)		Baryon	Octet Mass(MeV)	
			Our	Others		Our	Others
0.5		uud(p)	1065.68	939.00[11]	uds(Σ^0)	1344.67	1193.00[11]
0.7			967.41	938.27[51]		1239.94	1192.64[51]
1.0			931.08	866.00[52]		1203.29	1022.00[52]
1.5			924.27	938.27[1]		1195.98	1192.64[1]
0.5		ddu(n)	1067.24	939.00[11]	dds(Σ^-)	1345.46	1197.00[11]
0.7			971.74	939.57[51]		1243.71	1197.45[51]
1.0			935.77	866.00[52]		1205.99	1022.00[52]
1.5			929.04	939.56[1]		1199.06	1197.45[1]
0.5		uds(Λ^0)	1289.26	1116.00[11]	ssu(Ξ^0)	1420.19	1315.00[11]
0.7			1183.59	1115.68[51]		1331.65	1314.64[51]
1.0			1147.34	1022.00[52]		1297.09	1215.00[52]
1.5			1139.88	1115.68[1]		1291.43	1314.86[1]
0.5		uus(Σ^+)	1339.95	1189.00[11]	ssd(Ξ^-)	1428.97	1321.00[11]
0.7			1235.98	1189.39[51]		1340.44	1321.39[51]
1.0			1198.84	1022.00[52]		1306.55	1215.00[52]
1.5			1191.50	1189.37[1]		1299.61	1321.71[1]

Table 2. Masses of decuplet baryons ($J^P = \frac{3}{2}^+$)

hCPP $_{\nu}$	Baryon	Decuplet Mass(MeV)		Baryon	Decuplet Mass(MeV)	
		Our	Others		Our	Others
0.5	uuu(Δ^{++})	1361.68	1232.00[11]	uds(Σ^{*0})	1530.40	1384.00[11]
0.7		1264.17	1230.82[51]		1428.43	1384.18[51]
1.0		1228.63	1344.00[52]		1390.47	1447.00[52]
1.5		1221.21	1232.00[1]		1383.66	1383.70[1]
0.5	uud(Δ^+)	1358.3	1232.00[11]	dds(Σ^{*-})	1534.72	1387.00[11]
0.7		1260.78	1230.57[51]		1431.66	1387.18[51]
1.0		1223.74	1344.00[52]		1395.44	1447.00[52]
1.5		1216.33	1232.00[1]		1387.45	1387.20[1]
0.5	ddu(Δ^0)	1360.22	1232.00[11]	ssu(Ξ^{*0})	1640.49	1532.00[11]
0.7		1263.77	1231.87[51]		1549.05	1531.81[51]
1.0		1228.69	1344.00[52]		1516.19	1583.00[52]
1.5		1221.25	1232.00[1]		1508.03	1531.80[1]
0.5	ddd(Δ^-)	1356.79	1232.00[11]	ssd(Ξ^{*-})	1641.69	1535.00[11]
0.7		1260.32	1234.73[51]		1553.1	1534.95[51]
1.0		1223.65	1344.00[52]		1519.35	1583.00[52]
1.5		1217.80	1232.00[1]		1512.23	1535.00[1]
0.5	uus(Σ^{*+})	1534.60	1383.00[11]	sss(Ω^-)	1804.12	1672.00[11]
0.7		1430.54	1382.74[51]		1718.22	1672.45[51]
1.0		1392.93	1447.00[52]		1678.7	1701.00[52]
1.5		1386.16	1382.80[1]		1668.16	1672.45[1]

The computed magnetic moments of the octet and decuplet baryons are compared with the known experimental results as well as with other model predictions in Table 3 and 4 respectively. Present results for the choice of $\nu \approx 0.7$ are found to be in agreement with the known experimental values as well as with other model predictions. Here, it should be noted that the better agreement occur for the choice of ν ($0.6 \leq \nu \leq 0.7$) slightly below the saturation region ($\nu \geq 1$) (See Fig.1 - 4). However the experimental measurements of decuplet states are difficult and the known values for the Δ - baryons carry large errors [1, 2, 3].

The available experimental results for the Δ^{++} are 4.5 ± 0.95 and 3.5-7.5 are in very good agreement with our calculated magnetic moment 4.52 at $\nu = 0.7$. The calculated magnetic moments for Δ^+ , Δ^0 , and Ω^- are also in good agreement with experimental result while comparing with other theoretical models.

The behavior of the predicted magnetic moments of octet and decuplet baryons with potential index ν are shown in Fig.(3) and Fig.(4) respectively. The same satura-

Table 3. Magnetic moments of octet baryons (in μ_N)

Various models	p	n	Λ	Σ^+	Σ^0	Σ^-	Ξ^0	Ξ^-
hCPP $_{\nu}$								
$\nu = 1.5$	3.07	-2.04	-0.65	2.64	0.84	-0.98	-1.50	-0.55
$\nu = 1.0$	3.04	-2.07	-0.64	2.63	0.83	-0.98	-1.49	-0.55
$\nu = 0.7$	2.93	-1.93	-0.62	2.54	0.81	-0.95	-1.46	-0.54
$\nu = 0.5$	2.66	-1.76	-0.57	2.35	0.74	-0.88	-1.37	-0.51
EXPT. [1]	2.79	-1.91	-0.61	2.46		-1.16	-1.25	-0.65
QCDSR [26]	2.82	-1.97	-0.56	2.31	0.69	-1.16	-1.15	-0.64
χ CQM [29]	2.80	-2.11	-0.66	2.39	0.54	-1.32	-1.24	-0.50
χ PT [17]	2.58	-2.10	-0.66	2.43	0.66	-1.10	-1.27	-0.95
Latt [14]	2.79	-1.60	-0.50	2.37	0.65	-1.08	-1.17	-0.51
CDM [54]	2.79	-2.07	-0.71	2.47		-1.01	-1.52	-0.61
QM [55]	2.79	-1.91	-0.59	2.67	0.78	-1.10	-1.41	-0.47
QM+T [55]	2.79	-1.91	-0.61	2.39	0.63	-1.12	-1.24	-0.69
BAGCHI [11]	2.88	-1.91	-0.71	2.59	0.83	-0.92	-1.45	-0.62
Dai fit A [56]	2.84	-1.87		2.46		-1.06	-1.28	-0.61
Dai fit B [56]	2.80	-1.92		2.46		-1.23	-1.26	-0.63
SIMON [57]	2.54	-1.69	-0.69	2.48	0.80	-0.90	-1.49	-0.63
SU(3)BR. [58]	2.79	-1.97	-0.60	2.48	0.66	-1.16	-1.27	-0.65
PQM [53]	2.68	-1.99	-0.56	2.52		-1.17	-1.27	-0.59

tion trends towards saturation beyond the potential index $\nu > 1.0$ are observed. The shaded region in Fig.(3) corresponds to the region of ν ($0.6 < \nu < 0.7$) for which the predicted octet baryon magnetic moments show minimum root mean square deviation with the experiments. The predicted magnetic moments of the decuplet baryons in the same region of ν ($0.6 < \nu < 0.7$) are found to be closer to the existing experimental values of Δ and Ω baryons.

As the octet magnetic moments are known experimentally, we calculate the percentage variations of the different model predictions with respect to the experimental values and are given in Table 7 for comparison. The present $hCPP_{\nu \approx 0.7}$ prediction for p, n, Λ , Σ^+ baryons are much better with lesser percentage error compared to other model predictions. And the average percentage variations from proton to Ξ^- obtained from the Table 7 is about 8 % only, while that for the lattice predictions and that of χ PT predictions is about 10 and 11 % respectively. It can also be seen that the predictions of QCDSR and PQM are having lower variations of about 4 % only.

The transition magnetic moments obtained from the present study ($hCPP_{\nu}$ model) are in accordance with other theoretical predictions with much less variations with the

Table 4. Magnetic moments of decuplet baryons (in μ_N)

Various models	Δ^{++}	Δ^+	Δ^0	Δ^-	Σ^{*+}	Σ^{*0}	Σ^{*-}	Ξ^{*0}	Ξ^{*-}	Ω^-
hCPP $_{\nu}$										
$\nu = 1.5$	4.69	2.37	0.05	-2.34	2.61	0.29	-2.42	0.53	-1.92	-1.68
$\nu = 1.0$	4.66	2.35	0.05	-2.33	2.60	0.28	-2.40	0.53	-1.91	-1.67
$\nu = 0.7$	4.52	2.29	0.05	-2.25	2.53	0.27	-2.32	0.52	-1.87	-1.63
$\nu = 0.5$	4.19	2.12	0.05	-2.08	2.35	0.26	-2.15	0.49	-1.77	-1.56
Expt.	4.5 ± 0.95	$2.70^{+1.0}_{-1.3}$	≈ 0							-2.02 ± 0.06
[1, 2, 3]	3.5-7.5									
LCQCD [12]	4.40	2.20	0.00	-2.20	2.70	0.20	-2.28	0.40	-2.00	-1.56
QCDSR [13]	4.39	2.19	0.00	-2.19	2.13	0.32	-1.66	-0.69	-1.51	-1.49
Latt [14]	4.91	2.46	0.00	-2.46	2.55	0.27	2.02	0.46	-1.68	-1.40
χ PT [17]	6.04	2.84	-0.36	-3.56	3.07	0.00	-3.07	0.36	-2.56	-2.02
χ PT [18]	4.00	2.10	-0.17	-2.25	2.00	-0.07	-2.20	0.10	-2.00	input
RQM [22]	4.76	2.38	0.00	-2.38	1.82	-0.27	-2.36	-0.60	-2.41	-2.48
NRQM [24]	5.56	2.73	-0.09	-2.92	3.09	0.27	-2.56	0.63	-2.20	-1.81
χ QSM [27]	4.73	2.19	-0.35	-2.9	2.52	-0.08	-2.69	0.19	-2.48	-2.27
χ CQM [29]	4.51	2.00	-0.51	-3.02	2.69	0.02	-2.64	0.54	-1.84	-1.71
χ B [30]	3.59	0.75	-2.09	-1.93	2.35	-0.79	-3.87	0.58	-2.81	-1.75
EMS [49]	4.56	2.28	0.00	-2.28	2.56	0.23	-2.10	0.48	-1.90	-1.67
LCQCDSR[59]	6.34	3.17	0.00	-3.17						

choices of ν . However the experimentally known value for the transition magnetic moments of $(3.23 \pm 0.1) \Delta^0 \rightarrow n\gamma$ is higher than theoretical model predictions (see Table 5).

The parameter free predictions of the radiative decay width for $\Delta \rightarrow N\gamma$ ($N=n,p$) transitions obtained here are in very good agreement with experiment compared to other model predictions (see Table 6). Prediction for other decuplet to octet radiative transitions are well within the experimental limits.

At the end, we like to point out important feature of the $hCPP_{\nu}$ model is the saturation behaviour of the predicted properties of the baryons with $\nu > 1$. Similar saturation behaviour was also observed in the mass predictions of the $hCPP_{\nu}$ model in the heavy flavour sector [33].

It thus suggests that $hCPP_{\nu \geq 1}$ model can adequately represents the three body interactions among the quarks constituting the baryons.

Acknowledgement: The authors acknowledge the financial support from the Uni-

Table 5. Magnitude of the transition Magnetic moments ($|\mu_{\frac{3}{2}^+ \rightarrow \frac{1}{2}^+}|$) in μ_N

Decay Mode	Transition ($ \frac{3}{2}^+ \rightarrow \frac{1}{2}^+ $)	Magnetic moments (μ_N)		
		Expression	$hCPP_\nu$	others Expt. [3]
$\Delta^+ \rightarrow p\gamma$	$ \frac{2\sqrt{2}}{3}(\mu_u - \mu_d) $	$\nu = 0.5$	2.20	2.57 [60]
		$\nu = 0.7$	2.40	2.76 [61]
		$\nu = 1.0$	2.49	2.48 [49]
		$\nu = 1.5$	2.50	2.50 [9]
$\Delta^0 \rightarrow n\gamma$	$ - \frac{2\sqrt{2}}{3}(\mu_d - \mu_u) $	$\nu = 0.5$	2.23	2.57 [60]
		$\nu = 0.7$	2.42	2.76 [61] 3.23±0.1
		$\nu = 1.0$	2.51	2.58 [49]
		$\nu = 1.5$	2.52	2.50 [9]
$\Sigma^{*+} \rightarrow \Sigma^+\gamma$	$ \frac{2\sqrt{2}}{3}(\mu_u - \mu_s) $	$\nu = 0.5$	1.91	2.21 [60]
		$\nu = 0.7$	2.06	2.24 [61]
		$\nu = 1.0$	2.13	2.13 [49]
		$\nu = 1.5$	2.14	2.10 [9]
$\Sigma^{*0} \rightarrow \Sigma^0\gamma$	$ \frac{\sqrt{2}}{3}(2\mu_s - \mu_u - \mu_d) $	$\nu = 0.5$	0.89	0.88 [60]
		$\nu = 0.7$	0.97	1.01 [61]
		$\nu = 1.0$	1.00	0.96 [49]
		$\nu = 1.5$	1.01	0.89 [9]
$\Sigma^{*0} \rightarrow \Lambda^0\gamma$	$ \frac{\sqrt{2}}{\sqrt{3}}(\mu_u - \mu_d) $	$\nu = 0.5$	1.93	2.24 [60]
		$\nu = 0.7$	2.09	2.46 [61]
		$\nu = 1.0$	2.15	2.25 [49]
		$\nu = 1.5$	2.16	2.30 [9]
$\Sigma^{*-} \rightarrow \Sigma^-\gamma$	$ \frac{2\sqrt{2}}{3}(\mu_s - \mu_d) $	$\nu = 0.5$	0.21	0.44 [60]
		$\nu = 0.7$	0.22	0.22 [61]
		$\nu = 1.0$	0.23	0.22 [49]
		$\nu = 1.5$	0.23	0.31 [9]
$\Xi^{*0} \rightarrow \Xi^0\gamma$	$ \frac{2\sqrt{2}}{3}(\mu_u - \mu_s) $	$\nu = 0.5$	2.05	2.22 [60]
		$\nu = 0.7$	2.17	2.46 [61]
		$\nu = 1.0$	2.23	2.27 [49]
		$\nu = 1.5$	2.24	2.20 [9]
$\Xi^{*-} \rightarrow \Xi^-\gamma$	$ \frac{2\sqrt{2}}{3}(2\mu_s - \mu_d) $	$\nu = 0.5$	0.22	0.44 [60]
		$\nu = 0.7$	0.23	0.27 [61]
		$\nu = 1.0$	0.24	0.32 [49]
		$\nu = 1.5$	0.24	0.31 [9]

Table 6. Radiative decay widths (Γ_R in MeV) and branching ratio

Decay Mode	$hCPP_\nu$	Radiative Decay Width(Γ_R) in MeV			Branching Ratio in %		
		Our	Others	Expt.	Symbol	our	Expt. [1]
$\Delta^+ \rightarrow p\gamma$	$\nu = 0.5$	0.501	0.363 [60]			0.424	
	$\nu = 0.7$	0.601	0.430 [5]			0.510	
	$\nu = 1.0$	0.643	0.900 [9]	0.64 [62]	$\frac{\Gamma_R}{\Gamma(\Delta)}$	0.545	0.52-0.60
	$\nu = 1.5$	0.644				0.546	
$\Delta^0 \rightarrow n\gamma$	$\nu = 0.5$	0.517	0.363 [60]			0.438	
	$\nu = 0.7$	0.603	0.430 [5]			0.511	
	$\nu = 1.0$	0.655	0.900 [9]	0.64 [62]	$\frac{\Gamma_R}{\Gamma(\Delta)}$	0.555	0.52-0.60
	$\nu = 1.5$	0.655				0.555	
$\Sigma^{*+} \rightarrow \Sigma^+\gamma$	$\nu = 0.5$	0.111	0.100 [60]			0.310	
	$\nu = 0.7$	0.129	0.100 [5]			0.361	
	$\nu = 1.0$	0.137	0.11 [9]		$\frac{\Gamma_R}{\Gamma(\Sigma^{*+})}$	0.383	-
	$\nu = 1.5$	0.139				0.390	
$\Sigma^{*0} \rightarrow \Sigma^0\gamma$	$\nu = 0.5$	0.021	0.016 [60]			0.058	
	$\nu = 0.7$	0.026	0.017 [5]			0.072	
	$\nu = 1.0$	0.027	0.021 [9]	<1.750 [63]	$\frac{\Gamma_R}{\Gamma(\Sigma^{*0})}$	0.075	
	$\nu = 1.5$	0.027	0.022 [6]			0.077	
$\Sigma^{*0} \rightarrow \Lambda^0\gamma$	$\nu = 0.5$	0.216	0.241 [60]			0.600	
	$\nu = 0.7$	0.265				0.730	
	$\nu = 1.0$	0.274	0.470 [9]	<2.100 [64]	$\frac{\Gamma_R}{\Gamma(\Lambda^{*0})}$	0.763	1.3 \pm 0.4
	$\nu = 1.5$	0.279	0.275 [6]			0.776	
$\Sigma^{*-} \rightarrow \Sigma^-\gamma$	$\nu = 0.5$	0.001	0.004 [60]			0.003	
	$\nu = 0.7$	0.001	0.003 [5]			0.003	
	$\nu = 1.0$	0.001	0.002 [9]	< 0.009 [65]	$\frac{\Gamma_R}{\Gamma(\Sigma^{*-})}$	0.003	< 0.024
	$\nu = 1.5$	0.001				0.003	
$\Xi^{*0} \rightarrow \Xi^0\gamma$	$\nu = 0.5$	0.185	0.131 [60]			2.043	
	$\nu = 0.7$	0.200	0.129 [5]			2.197	
	$\nu = 1.0$	0.216	0.140 [9]		$\frac{\Gamma_R}{\Gamma(\Xi^{*0})}$	2.378	< 4.0
	$\nu = 1.5$	0.211				2.319	
$\Xi^{*-} \rightarrow \Xi^-\gamma$	$\nu = 0.5$	0.001	0.005 [60]			0.019	
	$\nu = 0.7$	0.002	0.003 [5]			0.021	
	$\nu = 1.0$	0.002	0.003 [9]		$\frac{\Gamma_R}{\Gamma(\Xi^{*-})}$	0.023	< 4.0
	$\nu = 1.5$	0.002				0.023	

Table 7. Percentage variation in the predictions of magnetic moments of octet baryons

system	$hCPP_\nu$ (In shaded region)	QCDSR [26]	χ CQM [29]	χ PT [17]	BAGCHI [11]	PQM [53]	LATTICE [14]
p	0.75	1.07	0.35	7.52	3.22	3.94	0.00
n	2.14	3.14	10.4	9.54	0.00	4.18	16.23
Λ	1.63	8.20	9.83	8.10	16.3	8.19	18.0
Σ^+	0.40	6.09	2.84	1.21	5.28	2.43	6.30
Σ^-	20.7	0.00	13.7	5.17	20.6	0.86	6.80
Ξ^0	13.6	8.00	0.80	0.00	16.0	1.60	6.40
Ξ^-	18.7	1.53	23.0	46.1	4.61	9.23	21.5
Average	8.20	4.00	8.70	11.00	9.43	4.34	10.74

versity Grant commission, Government of India under a Major research project F. 32-31/2006 (SR).

References

- [1] Amsler C *et al.* (Particle Data Group), Phys. Lett. **B 667**, 1 (2008).
- [2] M. Kotulla *et al.* Phys. Rev. Lett. **89**, 272001 (1991).
- [3] A. Bosshard *et al.*, Phys. Rev **D 44**, 1962 (1991).
- [4] W. M. Yao *et al.* (Particle Data Group), J. Phys. **G 33**, 1 (2006) and references therein.
- [5] D. B. Leinweber *et al.* Phys. Rev **D 48**, 2230 (1993).
- [6] E. Kaxiras *et al.* Phys. Rev **D 32**, 695 (1985) and references therein.
- [7] S. Capstick, Phys. Rev **D 46**, 1965 (1992).
- [8] M. N. Butler, M. J. Savage, and R. P. Springer, Nucl. Phys. **B 399**, 69 (1993).
- [9] T. M. Aliev and A. Ozpineci, Nucl. Phys. **B 732**, 291 (2006).
- [10] T. M. Aliev, K. Azizi and A. Ozpineci, Phys. Rev **D 79**, 056005 (2009).
- [11] M. Bagchi, S. Daw, M. Dey, and J. Dey, Europhys. Lett., **75**, 548 (2006).
- [12] T. M. Aliev and A. Ozpineci, Phys. Rev **D 62**, 053012 (2000).
- [13] Frank X. Lee, Phys. Rev **D 57**, 1801 (1998).
- [14] D. B. Leinweber, T. Draper, and R. M. Woloshyn, Phys. Rev. **D 46**, 3067 (1992).
- [15] I. C. Cloet, D. B. Leinweber and A. W. Thomas, Phys. Lett. **B 563**, 157 (2003).
- [16] I. C. Cloet, D. B. Leinweber and A. W. Thomas, arXiv:nucl-th/0211027
- [17] L. S. Geng, J. Martin Camalich, and M. J. Vicente Vacas, Chinese Physics **C 33**, X (2009); [arXiv:hep-ph/1001.0465].
- [18] M. N. Butler, M. J. Savage, and R. P. Springer, Phys. Rev. **D 49**, 3459 (1994).
- [19] Meissner and S. Steininger, Nucl. Phys. **B 499**, 349 (1997).
- [20] P. Ha and L. Durand, Phys. Rev. **D 58**, 093008 (1998).
- [21] S. J. Puglia and M. J. Ramsay, Phys. Rev. **D 62**, 034010 (2000).
- [22] F. Schlumpf, Phys. Rev. **D 48**, 4478 (1993).
- [23] K. T. Chao, Phys. Rev. **D 41**, 920 (1990).
- [24] Ha P. and Durand L., Phys. Rev. **D 58**, 093008 (1998).
- [25] Frank X. Lee, Phys. Lett. **B 419**, 14 (1998).
- [26] Lai Wang and Frank X. Lee, Phys. Rev. **D 78**, 013003 (2008).
- [27] H. C. Kim, M. Praszalowicz, and K. Goeke, Phys. Rev. **D 57**, 2859 (1998).

- [28] H. C. Kim, M. Praszalowicz, Phys. Lett. **B 585**, 99 (2004).
- [29] Harleen Dahiya, Neetika Sharma and P. K. Chatley [arXiv:hep-ph/0912.5256v1].
- [30] S. T. Hong and G. E. Brown, Nucl. Phys. **A 580**,408 (1994).
- [31] M. I. Krivoruchenko, Sov. J., Nucl. Phys. **A 45**,109 (1987).
- [32] Leinweber D. B., Draper T. and Woloshyn R. M., Phys. Rev. **D 46**, 3067 (1992).
- [33] Patel B, Rai A. K. and Vinodkumar P C, J. Phys. G, **35**, 065001 (2008).
- [34] Patel B, Majethiya A and Vinodkumar P C, Pramana - J. Phys. **72**, 679 (2009).
- [35] N.Isgur and G. Karl, Phys. Rev. **D 18**, 4187 (1978); 2653(1979); **D 20**, 1191 (1979); Phys. Lett. **B 72**, 109 (1977); Phys. Lett. **B 74**, 353 (1978).
- [36] S. Godfrey et al., Phys. Rev. **D 32**, 189 (1985).
- [37] S. Capstick and N. Isgur, Phys. Rev. **D 34**, 2809 (1986).
- [38] H. Dahiya and M. Gupta, Phys. Rev. **D 67**, 114015 (2003); M. Gupta and Navjot Kaur, Phys. Rev. **D 28**, 534 (1983); J. Singh and M. Gupta, J. Phys. **G 16**, L 45 (1990).
- [39] M. V. N. Murthy, Z. Phys. C-Particles and Fields **31**, 81-86 (1986).
- [40] W. Roberts and M. Pervin, [arXiv:hep-ph/0711.2492v1].
- [41] H Garcilazo, J Vijande and A Valcarce, J. Phys. **G 34**, 961-976 (2007).
- [42] R. Bijker, F. Iachello and A. Leviatan, Annals of Physics **284**, 89-133 (2000).
- [43] E. Santopinto, F. Iachello and M. M. Giannini, Eur. Phys. J. A **1**, 307- 315 (1998).
- [44] Majethiya A, Patel B, and P C Vinodkumar, Eur. Phys. J **A 42**, 213 (2009).
- [45] Sameer M. Ikhdaier and Ramazan Sever, Int. Jn. Mod. Phys. **A 21**, 3989 (2006); **18**, 4215 (2003); **19**, 1771 (2004); **21**, 2190 (2006).
- [46] K. Heikkila, N. A. Tornquist and S. Ono, Phys. Rev. **D 29**, 110 (1984).
- [47] X. T. Song, J. Phys. **G 17**, 49 (1991).
- [48] J. G. Contreras, R. Huerta, and L. R. Quintero, Revista Mexicana de Fisica **50**, 490 (2004).
- [49] Rohit Dhir and R. C. Verma, Eur. Phys. J **A 42**, 243 (2009).
- [50] Lang Yu *et al.* Phys. Rev. **D 66**, 033010 (2002) and references therein.
- [51] Phuoc Ha , J.Phys. **G 35**, 075006 (2008).
- [52] Mariaaline B. Do Vale *et al.*, Revista brasileira de Fisica **16**, 4 (1986).
- [53] J. Franklin, Phys. Rev. **D 73**, 114001 (2006).
- [54] Bae M. and McGovern J. A., J. Phys. **G 22**, 199 (1996).
- [55] S.K.Gupta and S.B.Khadkikar, Phys. Rev. **D 36**, 307 (1987).
- [56] Dai J., Dashen R., Jenkins E. and Manohar A. V., Phys. Rev. **D 53**, 273 (1996).
- [57] B. O. Kerbikov and Yu. A. Simonov, Phys. Rev. **D 62**, 093016 (2000).
- [58] J. W. Bos *et al.* Chinese J. of Phys. **35**, 2 (1997).
- [59] K. Azizi, Eur. Phys. J **C 61**, 311 (2009).
- [60] Lang Yu *et al.*, Phys. Rev. **D 73**, 114001 (2006).
- [61] S. T. Hong, Phys. Rev. **D 76**, 094029 (2007).
- [62] S. Eidelman *et al.*, Phys. Lett. **B 592**, 1 (2004).
- [63] J. Colas *et al.*, Nucl. Phys. **B 91**, 253 (1975).
- [64] T. S. Mast *et al.*, Phys. Rev. Lett. **21**, 1715 (1968).
- [65] V. V. Molchanov *et al.*, Phys. Lett. **B 590**, 161 (2004).